doi: 10.46793/EEE26-1.24H

Originalni naučni rad

UDK: 504.5:004.414.23

Simulations of Contaminant Dispersion from Accidental Releases in Cities: A CFD Approach

Mahir Hafizović[*], Muhamed Hadžiabdić[**], Bojan Ničeno[***]

[*] Enova LLC Consultants and Engineers Sarajevo, Bosnia and Herzegovina
[**] International University of Sarajevo, Bosnia and Herzegovina
[***] Paul Scherrer Institute, Switzerland

Abstract **-** Accidental releases of hazardous airborne contaminants in urban environments present a significant challenge for emergency response, risk assessment, and public safety, particularly in scenarios involving toxic or radiological substances. Accurate prediction of contaminant transport in densely built areas requires numerical tools capable of capturing the complex flow structures induced by urban geometry. Computational Fluid Dynamics (CFD) is widely used for this purpose, but its predictive accuracy depends strongly on the choice of turbulence modelling approach. This study evaluates hybrid RANS–LES (HRL) approach, for simulating contaminant dispersion from ground-level accidental releases in a realistic urban layout based on the wind tunnel experiment. Pollutant transport is analysed using mean and instantaneous flow and concentration fields, as well as experimental profiles, with particular emphasis on lateral spreading into adjacent streets, courtyards, and recirculation zones. Results show that HRL resolves unsteady vortex structures, producing pollutant transport patterns that closely match experimental observations. These findings underscore the importance of scale-resolving turbulence models for reliable prediction of accidental contaminant dispersion in urban areas and highlight the critical role of CFD in urban air quality assessment, emergency preparedness, and risk-informed decision-making.

Index Terms - Contaminant dispersion, Accidental releases, Urban air quality, Turbulence modelling, Computational Fluid Dynamics (CFD)

I INTRODUCTION

Urban areas present some of the most challenging environments for predicting airborne contaminant dispersion due to the complex interaction between atmospheric flow and three-dimensional building geometries. Accurate assessment of contaminant transport is essential for urban air quality management, risk assessment, and emergency preparedness, particularly in scenarios involving accidental releases of hazardous substances or radiological contaminants [1,2]. Traditional empirical or simplified dispersion models often lack the fidelity needed to capture the strong spatial variability in wind patterns and turbulent mixing induced by urban morphology [3,4]. This limitation has motivated increasing use of Computational Fluid Dynamics (CFD) in both research and practice of accidental hazardous releases in complex urban configurations [5,6,7,8]. CFD solves the governing equations of fluid motion and scalar transport with spatial resolution, enabling the prediction of localized flow features that control dispersion. Over the past decade, numerous studies have demonstrated its potential for urban applications. While early work focused on isolated structures, contemporary research highlights the ability of CFD to resolve airflow within complex street canyons and real-city geometries. [9,10]. Nonetheless, the reliability of CFD predictions remains highly dependent on the choice of turbulence modelling.

Steady Reynolds-averaged Navier–Stokes (RANS) models remain common in industry due to their low computational cost, but they often struggle to represent the unsteady turbulent structures that govern mixing near sharp edges and variable building arrangements [9,11]. Large-eddy simulation (LES), conversely, explicitly resolves larger energy-containing turbulent motions and has shown excellent agreement with wind-tunnel and field measurements [12,13]. However, pure LES remains computationally demanding for urban-scale applications. Hybrid approaches that combine RANS and LES offer a pragmatic compromise. These frameworks resolve key unsteady structures in the urban canopy while retaining numerical efficiency in the far-field.

The relevance of high-fidelity urban dispersion modelling is particularly pronounced in the context of nuclear energy systems. While large-scale regional dispersion is typically addressed using mesoscale atmospheric models, near-field and neighbourhood-scale transport within the first few kilometres of a release remains strongly influenced by local geometry, surface roughness, and built structures. In such cases, simplified Gaussian or integral plume models may not adequately capture the spatial variability of exposure within complex environments.

This challenge becomes increasingly important with the anticipated deployment of Small Modular Reactors (SMRs). Unlike traditional large nuclear power plants, which are typically located in remote or low-density areas, SMRs are being designed for greater siting flexibility, including potential installation near industrial zones, district heating networks, or even peri-urban and urban environments. In these contexts, accidental releases, however unlikely, would interact directly with surrounding buildings, transportation corridors, and densely populated districts. Accurate prediction of short-range dispersion, recirculation, and pollutant accumulation zones becomes essential for emergency preparedness, evacuation planning, and shelter-in-place strategies.

In this context, the present study applies a hybrid RANS-LES methodology to simulate atmospheric flow and pollutant dispersion within a semi-idealized urban layout. Beyond model validation, the study emphasizes the practical value of CFD for urban risk assessment and emergency planning. By identifying areas prone to pollutant accumulation and pathways that facilitate flushing, CFD provides actionable insight for designing evacuation routes and supporting real-time operational decisions in accidental release scenarios.

II METHODOLOGY

The analysis of contaminant dispersion is conducted using the CFD methodology. This approach solves the full set of Navier-Stokes equations governing the three-dimensional motion of fluid, together with transport equations for gas tracer concentration and turbulence properties. By employing numerical techniques, detailed distributions of velocity, pressure, concentration, and turbulent variables are obtained throughout the computational domain.

The simulations adopt a field-based approach, in which velocity, concentration and turbulent variables are computed simultaneously and interactively within a time-dependent, three-dimensional framework. A computational mesh with appropriate spatial and temporal resolution is utilized to capture the time evolution of flow patterns and tracer gas dispersion across the entire solution domain.

The Navier-Stokes and the concentration transport equations in the RANS framework read:

$$\frac{\partial U_i}{\partial x_i} = 0,$$

$$\frac{DU_i}{Dt} = -\frac{1}{\rho}\frac{\partial P}{\partial x_i} + \frac{\partial}{\partial x_j}\left(\nu\left(\frac{\partial U_i}{\partial x_j} + \frac{\partial U_j}{\partial x_i}\right) - \overline{u_i u_j}\right) + g_i$$

$$\frac{DC}{Dt} = \frac{\partial}{\partial x_j}\left(\frac{\nu}{Sc}\frac{\partial C}{\partial x_j} - \overline{c u_j}\right) + S_c$$

where U_i is velocity vector, ρ is fluid density, g_i is gravity vector, ν is kinematic viscosity, C is concentration, and Sc is Schmidt number.

The momentum and concentration equations are closed by the linear eddy-viscosity/diffusivity formulation:

$$\overline{u_i u_j} = -\nu_t S_{ij} + 2k\delta_{ij}/3, \qquad \overline{c u_j} = -\frac{\nu_t}{Sc_t}\frac{\partial C}{\partial x_j}$$

Where ν_t is turbulent (eddy) viscosity, and Sc_t turbulent Schmidt number set to its standard value of 0.9.

Turbulence modelling is based on the elliptic-relaxation hybrid RANS-LES approach (ER-HRL) by [14], employing the k-ε-ζ-f (or simply ζ-f) by [15] in the RANS region and the dynamic Smagorinsky model [16] in the LES region. This turbulence model has been extensively validated against numerous benchmark cases, ensuring its reliability and predictive accuracy [9, 17-20].

The ζ-f model in its original form consists of the following equations, applied also in the ensemble-averaged framework:

$$\frac{Dk}{Dt} = \mathcal{D}_k + P_k - \varepsilon$$

$$\frac{D\varepsilon}{Dt} = \mathcal{D}_\varepsilon + \frac{c_{\varepsilon 1}P_k - c_{\varepsilon 2}\varepsilon}{\tau}$$

$$\frac{D\zeta}{Dt} = \mathcal{D}_\zeta + f - \frac{\zeta}{k}P_k$$

$$L^2\nabla^2 f - f = \frac{1}{\tau}\left(c_1 + c_2'\frac{P_k}{\varepsilon}\right)\left(\zeta - \frac{2}{3}\right)$$

$$\tau = max\left[min\left(\frac{k}{\varepsilon}, \frac{0.6}{\sqrt{6}c_\mu^\upsilon |S|\zeta}\right), c_\tau\left(\frac{\nu}{\varepsilon}\right)^{1/2}\right]$$

$$L = C_L max\left[min\left(\frac{k^{\frac{3}{2}}}{\varepsilon}, \frac{k^{\frac{1}{2}}}{\sqrt{6}c_\mu^\upsilon |S|\zeta}\right), c_\eta\left(\frac{\nu^3}{\varepsilon}\right)^{\frac{1}{4}}\right]$$

$$\nu_t = c_\mu^\upsilon\, \zeta\, k\, \tau$$

where k is the RANS ensemble modelled turbulent kinetic energy, ε its dissipation rate, $P_k = \overline{u_i u_j}\frac{\partial U_i}{\partial x_j}$ is the production rate of turbulent kinetic energy, ζ=v^2/k is the velocity scale ratio, f is an elliptic relaxation function and $\mathcal{D}$ denotes the total (molecular plus turbulent) diffusion:

$$\mathcal{D}_\phi = \frac{\partial}{\partial x_k}\left[\left(\frac{\nu}{\sigma_\phi} + \frac{\nu_t}{\sigma_t}\right)\frac{\partial \Phi}{\partial x_k}\right]$$

The details on the switching between the RANS and LES region for the ER-HRL model can be found in [14].

Wall boundary conditions for all variables are prescribed within the grid cells nearest to solid surfaces, positioned beyond the viscous sub-layer. This is achieved through the application of semi-empirical wall functions, which are derived by pre-integrating the governing equations over near-wall grid cells.

The computations were conducted using the in-house finite-volume unstructured T-Flows CFD code (https://github.com/DelNov/T-Flows), developed at TU Delft by [21,22]. T-Flows has been extensively tested and validated against multiple benchmark cases relevant to the present configurations by [9,17-20, 23-26].

III REFERENCE EXPERIMENT AND APPROACH FLOW SIMULATION

The numerical study is based on the Michelstadt wind-tunnel experiment conducted at the University of Hamburg within COST Action ES1006 [27,28]. The experiment represents a semi-idealized Central European urban layout and provides a well-documented dataset for validating urban flow and pollutant dispersion models.

The physical model consists of 60 flat-roof buildings with internal courtyards and three representative heights (15 m, 18 m, and 24 m at full scale), Fig. 1a. A continuous point source of tracer gas is located in an open area within the domain. The experimental database includes detailed measurements of mean streamwise and spanwise velocity components and turbulence intensity at 40 locations, and tracer gas concentration at multiple vertical and horizontal profiles across the urban canopy.

In the wind tunnel, an atmospheric boundary layer was generated using vertical spires and rows of roughness elements to reproduce realistic urban inflow conditions, Fig. 1b. To replicate these conditions numerically, a periodic precursor channel simulation was performed to generate a representative turbulent inflow profile, Fig. 3a. Instead of explicitly modelling all roughness elements, a simplified resistance-based approach [17] was adopted to reproduce their overall flow effects while maintaining reasonable computational cost. The total cell count of the precursor simulation was approximately 300,000, Fig. 2.

The bottom boundary was treated as a no-slip wall, while a symmetry boundary condition was imposed at the top. The mass flow rate was adjusted to match the experimental reference velocity of U_{ref} = 6 m/s at a reference height of 100 m.

The ER-HRL turbulence model was applied, and statistics were collected over 10,000 time-steps after reaching a statistically stationary state, with a physical time step of 0.5 s.

(a)

(b)

Figure 1. Wind tunnel configuration. (a) Test section with buildings and white rectangular obstacles placed downstream of the inflow. (b) Plan view showing the tracer gas inlet (red square); eight upstream vertical spires generate the turbulent boundary layer

Comparison with measurements shows very good agreement for the mean wind profile, Fig. 3b. Turbulence levels were moderately underestimated, which is expected given the simplified representation of complex wind-tunnel roughness elements. A higher-resolution simulation using 1.3 million cells improved turbulence prediction but at significantly higher computational cost. Since the objective of this study is to develop a practical and transferable approach for urban-scale applications, a balanced configuration was retained.

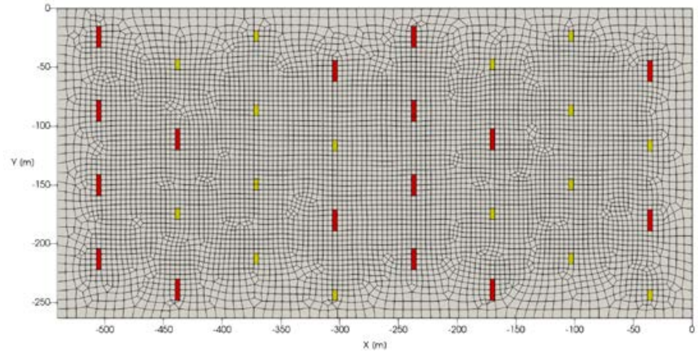

Figure 2. Numerical mesh employed for the precursor simulation (red squares indicate high obstacles (18 m), while yellow squares denote short obstacles (9 m))

(a)

(b)

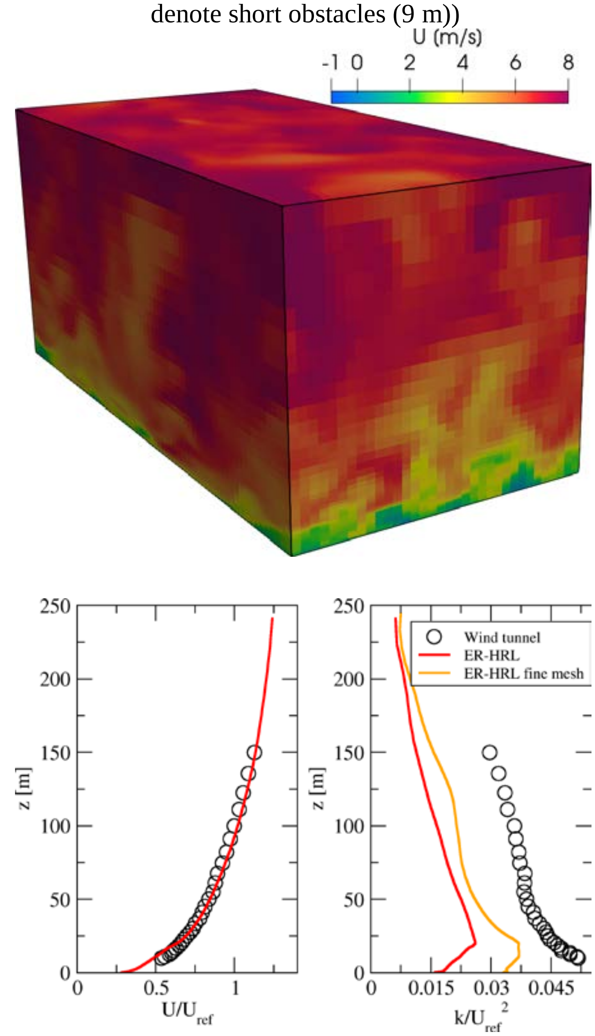

Figure 3. Precursor simulation results: (a) instantaneous streamwise velocity field within the precursor domain; (b) mean inlet profiles of normalized streamwise velocity and turbulent kinetic energy extracted from the precursor simulation compared to experimental data

To compensate for lower inflow turbulence, additional upstream roughness elements were introduced in the main domain, as presented in the following section. Previous studies [29, 30] indicate that urban flows rapidly adjust within the first building rows, and that simplified inflow treatments can provide comparable accuracy for predicting building-scale wind patterns and pollutant dispersion.

IV Computational domain and numerical details

The computational domain representing the urban area has overall dimensions of 85H × 37.5H × 10H (H = maximum building height), Fig. 4. Building colours indicate height (white: 15 m, orange: 18 m, red: 24 m). Green elements represent porosity-modelled obstacles. Red dot represents a pollution source. The inlet is positioned sufficiently upstream of the first building row to allow additional roughness elements to sustain turbulence, while adequate spacing is also provided downstream and laterally, consistent with the original wind-tunnel configuration. The vertical extent of the domain exceeds standard steady-state recommendations [31] in order to accommodate large turbulent structures typical of scale-resolving simulations and to minimize artificial boundary effects.

The mesh was designed to provide enhanced resolution in regions where strong gradients and mixing processes occur, Fig. 5. The red square represents the pollution source. Around the pollutant source, a horizontal resolution of approximately 1 m was applied to accurately capture near-source concentration fields.

Within street canyons, the typical horizontal cell size is about 3 m, while in courtyards it is approximately 4-5 m. In the vertical direction, the near-ground region was refined using stretched layers to better resolve shear and turbulence generation close to surfaces, with progressively coarser spacing toward the top of the domain. The total grid consists of approximately 3.25 million cells.

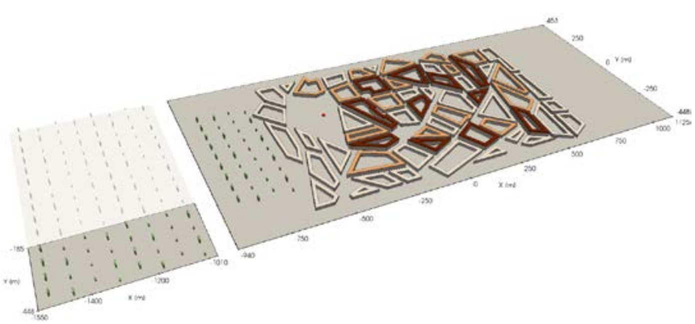

Figure 4. Precursor and computational domains

A simultaneous precursor-main domain strategy was employed. Turbulent inflow data generated in the precursor simulation were transferred dynamically to the inlet of the urban domain, ensuring realistic and time-varying boundary conditions.

After an initial spin-up period to allow the flow to fully develop across the domain, statistical averages were collected over an extended simulation period. The pollutant release was modelled as a continuous vertical emission corresponding to the experimental flow rate. Standard no-slip conditions were applied at solid surfaces, and air properties representative of typical ambient conditions were assumed. A physical time step of 0.2 s was used. Pressure-velocity coupling was handled using the SIMPLE algorithm.

Figure 5. Computational mesh used in simulations

V Results and discussion

The simulated pedestrian-level flow field clearly reflects the influence of urban morphology, Fig. 6a. High wind speeds are mainly confined to large open areas and elongated passages aligned with the prevailing wind, which act as natural ventilation corridors. In contrast, dense building clusters and enclosed courtyards exhibit pronounced velocity deficits, including stagnation zones and recirculation regions. The strongest recirculation occurs in deep street canyons oriented perpendicular to the approaching wind and within small courtyards surrounded by taller buildings. Overall, the near-ground flow is highly heterogeneous, characterized by alternating well-ventilated pathways and sheltered low-momentum zones.

(a)

(b)

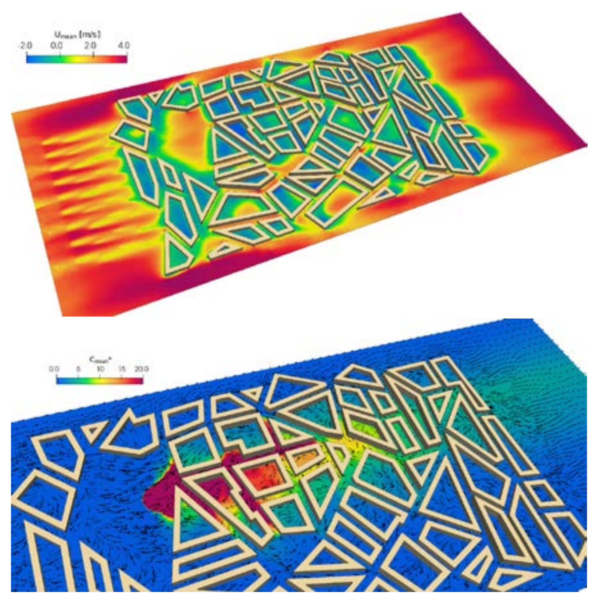

Figure 6. Fields of instantaneous (a) streamwise velocity and (b) concentration in horizontal slice at 1.8 m

The concentration field strongly follows these flow patterns, Fig. 6b. A pronounced hotspot forms near the emission source within a semi-enclosed courtyard, where weak ventilation allows pollutants to accumulate. Rather than dispersing uniformly, the plume spreads preferentially along wind-aligned corridors and gradually penetrates adjacent streets through localized high-velocity gaps. A clear inverse relationship is observed between mean wind speed and pollutant concentration: areas with near-zero velocities exhibit the highest concentrations, while well-ventilated zones experience substantial dilution.

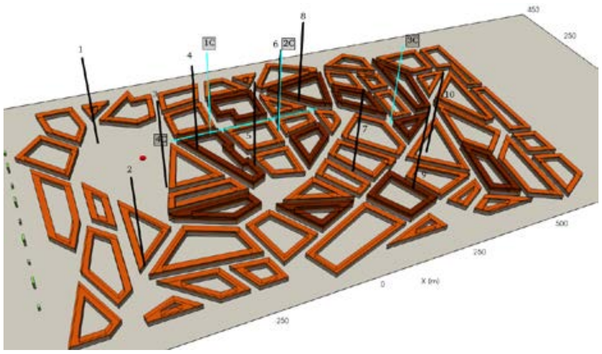

Figure 7. Location of the selected profiles for comparison with experimental results

Figure 7 shows locations of ten selected vertical and horizontal profiles where streamwise and spanwise velocity, turbulent kinetic energy, and concentration measurements within the urban canopy are available. The black lines represent available vertical profiles for velocity components and turbulent kinetic energy (1-10), while blue lines represent vertical and horizontal profiles for pollutant concentration (1C-4C).

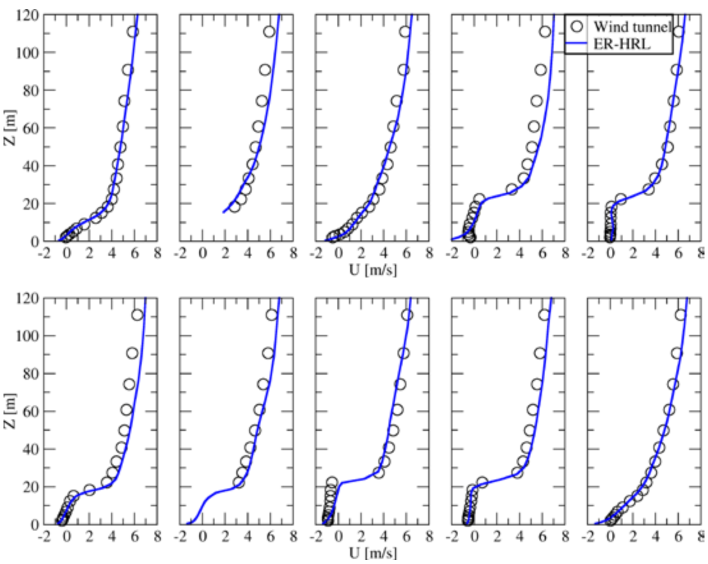

Figure 8. Comparison of predicted and experimental streamwise velocity profiles at ten selected measurement locations within the domain

Within the canopy layer, the streamwise velocity exhibits strong spatial variability, Fig. 8. In dense building clusters and leeward zones, near-ground velocities are close to zero and may become slightly negative, indicating recirculation and shielding effects. In contrast, more open locations show a smoother increase of velocity with height, reflecting better exposure to the approaching flow and improved vertical connectivity. A clear inflection point appears around roof level, marking the transition from the geometry-dominated canopy flow to the more uniform atmospheric boundary layer above, where the direct influence of individual buildings rapidly diminishes.

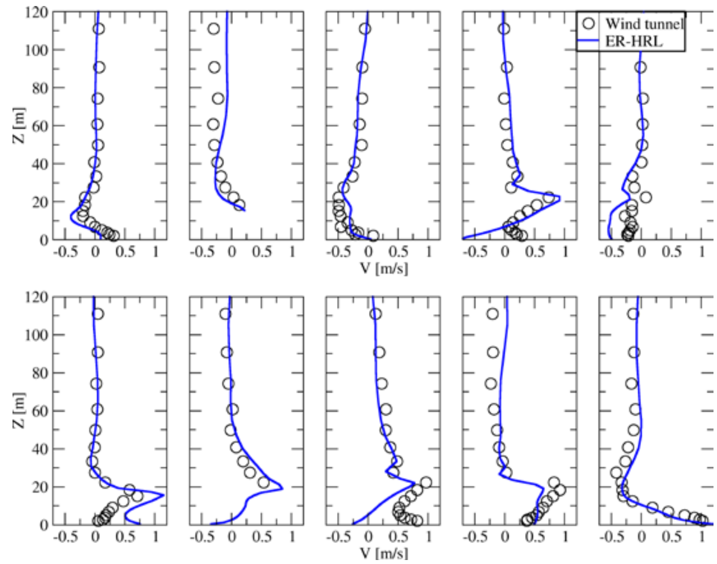

Figure 9. Comparison of predicted and experimental spanwise velocity profiles at ten selected measurement locations within the domain

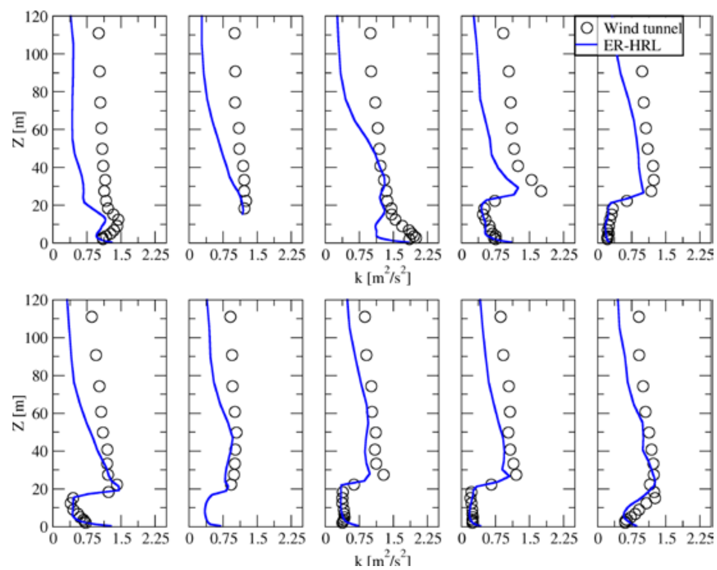

Figure 10. Comparison of predicted and experimental turbulent kinetic energy profiles at ten selected measurement locations within the domain

The spanwise (lateral) velocity component highlights the inherently three-dimensional character of urban ventilation, Fig. 9. While mean lateral velocities tend to approach zero above roof height, significant deviations occur within the canopy, particularly in areas with staggered or irregular building arrangements. These cross-flows enable exchange between adjacent streets and courtyards, demonstrating that pollutant redistribution depends not only on streamwise transport but also on lateral mixing pathways within the urban fabric.

Profiles of turbulent kinetic energy (TKE), Fig. 10, consistently show maxima near roof level. This peak corresponds to the shear layer formed by flow separation at building tops and the interaction between slow canopy air and the faster overlying flow. Below roof height, especially within deep or narrow street canyons, turbulence intensity decreases substantially toward the ground. The reduced turbulence limits vertical exchange and weakens mixing at pedestrian level, increasing the likelihood of pollutant accumulation in sheltered zones.

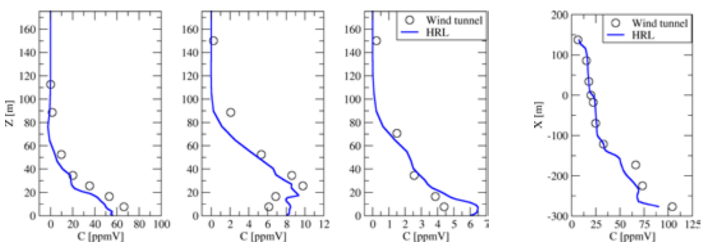

Figure 11. Comparison of predicted and experimental concentration profiles along three vertical transects and one horizontal transect within the measurement domain

The concentration profiles reflect this vertical structure, Fig. 11. Elevated pollutant levels persist throughout the canopy and decay gradually with height, indicating limited dilution within the built environment. Above roof level, concentrations decrease sharply as the plume enters the more energetic outer flow, where higher wind speeds and turbulence enhance dispersion. The roof-shear layer therefore acts as the primary ventilation interface controlling vertical pollutant removal from the urban canopy.

VI Conclusions

This study demonstrates that CFD, when coupled with appropriate turbulence modelling, is a powerful and essential tool for predicting contaminant dispersion in complex urban environments. The hybrid RANS–LES approach used here provides reliable predictions of pollutant transport, capturing the effects of urban geometry on both horizontal and vertical dispersion while remaining computationally feasible for realistic city-scale applications.

From a practical standpoint, the findings are highly relevant for emergency preparedness and response planning. In accidental release scenarios, whether involving hazardous industrial chemicals, transportation-related spills, or radiological contaminants as observed in major nuclear accidents, exposure patterns are governed by the interaction between atmospheric flow and urban morphology. This aspect becomes particularly important in the context of next-generation nuclear technologies, such as SMRs, which are expected to offer greater siting flexibility and may be deployed closer to industrial hubs or urban infrastructure networks. In such settings, accurate near-field dispersion modelling is critical. CFD-based simulations enable identification of stagnation zones, ventilation corridors, and high-risk accumulation areas at pedestrian height, thereby supporting evacuation planning, definition of exclusion zones, placement of monitoring systems, and real-time operational decision-making.

Overall, the study confirms that advanced CFD approaches, supported by validated turbulence models, should be considered a core component of modern urban risk assessment and resilience planning. As cities grow denser and infrastructure systems become more interconnected, predictive, physics-based tools will play an increasingly central role in safeguarding public health and guiding evidence-based emergency management strategies.

References

[1] Bartzis, J. G., Sakellaris, I. A., Efthimiou, G. On exposure uncertainty quantification from accidental airborne point releases, Journal of Hazardous Materials Advances, Vol. 6, 100080, 2022. https://doi.org/10.1016/j.hazadv.2022.100080

[2] Bartzis, J. G., Sakellaris, I. A., Andronopoulos, S., Venetsanos, A., Triantafyllou, A. Towards new simplified methodologies on source term estimation and associated uncertainties from accidental airborne releases, Building and Environment, Vol. 251, 111222, 2024. https://doi.org/10.1016/j.buildenv.2024.111222

[3] Miao, Y., Liu, S., Zheng, H., Zheng, Y., Chen, B., Wang, S. A multi-scale urban atmospheric dispersion model for emergency management, Advances in Atmospheric Sciences, Vol. 31, No. 6, pp. 1353-1365, 2014. https://doi.org/10.1007/s00376-014-3254-9

[4] Rentai, Y.A.O. Atmospheric dispersion of radioactive material in radiological risk assessment and emergency response, Progress in Nuclear Science and Technology, Vol. 1, pp. 7-13, 2011. https://www.aesj.net/document/pnst001/7.pdf [pristupljeno 12.01.2026]

[5] Pontiggia, M., Derudi, M., Alba, M., Scaioni, M., Rota, R. Hazardous gas releases in urban areas: Assessment of consequences through CFD modelling, Journal of hazardous materials, Vol. 176, No. 1-3, pp. 589-596, 2010. https://doi.org/10.1016/j.jhazmat.2009.11.070

[6] Sanchez, E.Y., Lerner, J.C., Porta, A., Jacovkis, P. M. Accidental release of chlorine in Chicago: Coupling of an exposure model with a Computational Fluid Dynamics model, Atmospheric environment, Vol. 64, pp. 47-55, 2013. https://doi.org/10.1016/j.atmosenv.2012.09.037

[7] Armand, P., Oldrini, O., Duchenne, C., Perdriel, S. Topical 3D modelling and simulation of air dispersion hazards as a new paradigm to support emergency preparedness and response, Environmental Modelling & Software, Vol. 143, 105129, 2021. https://doi.org/10.1016/j.envsoft.2021.105129

[8] Mendil, M., Leirens, S., Armand, P., Duchenne, C. Hazardous atmospheric dispersion in urban areas: A Deep Learning approach for emergency pollution forecast, Environmental Modelling & Software, Vol. 152, 105387, 2022. https://doi.org/10.1016/j.envsoft.2022.105387

[9] Hadžiabdić, M., Hafizović, M., Ničeno, B., Hanjalić, K. A rational hybrid RANS-LES model for CFD predictions of microclimate and environmental quality in real urban structures, Building and Environment, Vol. 217, 109042, 2022. https://doi.org/10.1016/j.buildenv.2022.109042

[10] Zhang, Y., Ye, X., Wang, S., He, X., Dong, L., Zhang, N., Xiao, Y. Large-eddy simulation of traffic-related air pollution at a very high resolution in a mega-city: evaluation against mobile sensors and insights for influencing factors, Atmospheric Chemistry and Physics, Vol. 21, No. 4, pp. 2917-2929, 2021. https://doi.org/10.5194/acp-21-2917-2021

[11] Liu, J., Niu, J. CFD simulation of the wind environment around an isolated high-rise building: An evaluation of SRANS, LES and DES models, Building and Environment, Vol.96, pp. 91-106, 2016. https://doi.org/10.1016/j.buildenv.2015.11.007

[12] Ono, A., Nozu, T. Comparison between wind tunnel experiment and large-eddy simulation of concentration fluctuations in pollutant dispersion in a realistic urban area, Journal of Wind Engineering and Industrial Aerodynamics, Vol. 253, 105832, 2024. https://doi.org/10.1016/j.jweia.2024.105832

[13] García-Sánchez, C., Van Beeck, J., Gorlé, C. Predictive large eddy simulations for urban flows: Challenges and opportunities, Building and Environment, Vol. 139, pp. 146-156, 2018. https://doi.org/10.1016/j.buildenv.2018.05.007

[14] Hadziabdic, M. LES, *RANS and combined simulation of impinging flows and heat transfer*, University of Sarajevo, Bosnia and Herzegovina, 2005.

[15] Hanjalić, K., Popovac, M., Hadžiabdić, M. A robust near-wall elliptic-relaxation eddy-viscosity turbulence model for CFD, International journal of heat and fluid flow, Vol. 25, No. 6, pp. 1047-1051, 2004. https://doi.org/10.1016/j.ijheatfluidflow.2004.07.005

[16] Germano, M., Piomelli, U., Moin, P., Cabot, W. H. A dynamic subgrid-scale eddy viscosity model, Physics of fluids a: Fluid dynamics, Vol. 3, No. 7, pp. 1760-1765, 1991. https://doi.org/10.1063/1.857955

[17] Hadziabdic, M., Hodza, A., Niceno, B. Modelling urban canopy with object-based porosity model, International Journal of Heat and Fluid Flow, Vol. 107, 109394, 2024. https://doi.org/10.1016/j.ijheatfluidflow.2024.109394

[18] Hadziabdic, M., Niceno, B. Reconstruction of Nusselt number in RANS computations with wall function approach, Nuclear Engineering and Design, Vol. 412, 112461, 2023. https://doi.org/10.1016/j.nucengdes.2023.112461

[19] Hanjalić, K., Laurence, D., Popovac, M., Uribe, J. $v2/k - f$ Turbulence model and its application to forced and natural convection. In: Rodi, W., Mulas, M. (Eds.), *Engineering Turbulence Modelling and Experiments*, Vol. 6. Elsevier Science B.V., pp. 67-76, 2005. https://doi.org/10.1016/b978-008044544-1/50005-4 00

[20] Delibra, G., Hanjalic, K., Borello, D., Rispoli, F. Vortex structures and heat transfer in a wall bounded pin matrix: LES with a RANS wall treatment, International Journal of Heat Fluid Flow, Vol 31, No. 5, pp. 740-753, 2010. https://doi.org/10.1016/j.ijheatfluidflow.2010.03.004

[21] Niceno, B. *An Unstructured Parallel Algorithm for Large Eddy and Conjugate Heat Transfer Simulations*, PhD thesis, Delft University of Technology, Delft, Netherlands, 2001.

[22] Niceno, B., Hanjalic, K. Unstructured large-eddy and conjugate heat transfer simulations of wall-bounded flows, in: S. Sunden, M. Faghri (Eds.), *Modelling and Simulation of Turbulent Heat Transfer*, WIT Press, USA, pp. 35-76, 2005.

[23] Palkin, E., Hadziabdic, M., Mullyadzhanov, R., Hanjalic, K. Control of flow around a cylinder by rotary oscillations at a high subcritical Reynolds number, Journal of Fluid Mechanics, Vol. 855, pp. 236-266, 2018. https://doi.org/10.1017/jfm.2018.639

[24] Van Reeuwijk, M., Hadziabdic, M. Modelling high Schmidt number turbulent mass transfer, International Journal of Heat Fluid Flow, Vol. 51, pp. 42-49, 2015. https://doi.org/10.1016/j.ijheatfluidflow.2014.10.025

[25] Temmerman, L., Hadziabdic, M., Leschziner, M.A., Hanjalic, K. A hybrid two-layer URANS–LES approach for large eddy simulation at high Reynolds numbers, International Journal of Heat Fluid Flow, Vol. 26, No. 2, pp. 173-190, 2005. https://doi.org/10.1016/j.ijheatfluidflow.2004.07.006

[26] Hafizović, M., Hadžiabdić, M., Ničeno, B. Numerical Simulations of Heat Transfer in Underground Thermal Energy Storage (UTES) System: CFD Approach, Energetika, Ekonomija, Ekologija, Vol. 27, No. 1, pp. 24-31, 2005. https://doi.org/10.46793/EEE25-1.24H

[27] COST, ES1006 - Evaluation, improvement and guidance for the use of local-scale emergency prediction and response tools for airborne hazards in built environments. https://www.cost.eu/actions/ES1006/ [pristupljeno 28.01.2026]

[28] Berbekar, E., Harms, F., Leitl, B. Wind-tunnel measurements of accidental gas releases in a simplified urban environment, in Proc. *HARMO, 16th International Conference on Harmonisation within Atmospheric Dispersion Modelling for Regulatory Purposes*, Varna, Bulgaria, 8-11 September, 2014.

[29] Ricci, A., Kalkman, I., Blocken, B., Burlando, M., Freda, A., Repetto, M. P. Large-scale forcing effects on wind flows in the urban canopy: Impact of inflow conditions, Sustainable cities and Society, Vol. 42, pp. 593-610, 2018. https://doi.org/10.1016/j.scs.2018.08.012

[30] An, K., Fung, J. C. H., Yim, S. H. L. Sensitivity of inflow boundary conditions on downstream wind and turbulence profiles through building obstacles using a CFD approach, Journal of Wind Engineering and Industrial Aerodynamics, Vol. 115, pp. 137-149, 2013. https://doi.org/10.1016/j.jweia.2013.01.004

[31] Franke, J., Hirsch, C., Jensen, A. G., Krüs, H. W., Schatzmann, M., Westbury, P. S., Miles, S.D., Wisse, J.A., Wright, N. G. Recommendations on the use of CFD in predicting pedestrian wind environment, Cost action C, Vol. 14, pp. 1-12, 2004.

Authors

Mahir Hafizović – MSc., Enova LLC / International University of Sarajevo – Mechanical Eng. Department, mahir.hafizovic@enova.ba, ORCID 0000-0002-9319-6932

Muhamed Hadžiabdić – Prof. Dr., International University of Sarajevo – Mechanical Eng. Department, mhadziabdic@ius.edu.ba, ORCID 0000-0002-2726-3914

Bojan Ničeno – Dr., Senior Scientist, Paul Scherrer Institute – Nuclear Energy and Safety Department, bojan.niceno@psi.ch, ORCID 0000-0002-8583-1684

Simulacije širenja zagađujućih materija uslijed nenamjernih ispuštanja u gradovima: CFD pristup

Rezime - *Slučajna ispuštanja opasnih zagađujućih materija u urbanim sredinama predstavljaju značajan izazov za hitne službe, procjenu rizika i javnu sigurnost, posebno u scenarijima koji uključuju toksične ili radioaktivne materije. Precizno predviđanje transporta zagađujućih materija u gusto izgrađenim područjima zahtijeva numeričke alate sposobne da reproduciraju složene tokove uzrokovane urbanom geometrijom. Za ovu svrhu se široko koristi računska dinamika fluida (eng. Computational Fluid Dynamics, CFD), ali njena tačnost uveliko zavisi od izbora pristupa modeliranju turbulencije.*

Ova studija ispituje hibridni RANS–LES (HRL) pristup za simulaciju širenja zagađujućih materija u realnom gradskom okruženju, zasnovanom na eksperimentu u zračnom tunelu. Transport zagađujućih materija analiziran je korištenjem srednjih i trenutnih polja brzine i koncentracije, kao i eksperimentalnih profila, s posebnim naglaskom na lateralno širenje u susjedne ulice, dvorišta i zone recirkulacije.

Rezultati pokazuju da HRL može predvidjeti nestacionarne vrtložne strukture, stvarajući obrasce širenja zagađujućih materija koji se vrlo dobro poklapaju s eksperimentalnim rezultatima. Ovi rezultati naglašavaju važnost modela turbulencije sposobnih da reproduciraju nestacionarne strukture toka za pouzdano predviđanje širenja zagađujućih materija u gradovima i naglašavaju ključnu ulogu CFD-a u procjeni kvaliteta zraka, pripremi za hitne situacije i donošenju odluka zasnovanih na riziku.

Ključne reči - *Disperzija zagađujućih materija, slučajna ispuštanja, kvalitet zraka, modeliranje turbulencije, računska dinamika fluida*

Rad primljen 15.01.2026., prihvaćen 01.03.2026.